Journal Pre-proof

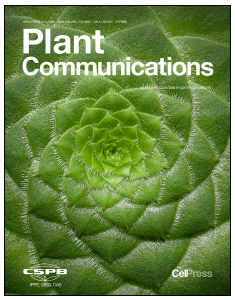

Multi-omics analysis reveals distinct responses to light stress in photosynthesis and primary metabolism between maize and rice

Fengying Duan, Xia Li, Ze Wei, Jing Li, Caifu Jiang, Chengzhi Jiao, Shanshan Zhao, Yu Kong, Mengxiao Yan, Jirong Huang, Jun Yang, Yanmei Chen, Ralph Bock, Wenbin Zhou

PII: S2590-3462(25)00250-0

DOI: https://doi.org/10.1016/j.xplc.2025.101488

Reference: XPLC 101488

To appear in: *Plant Communications*

Received Date: 22 January 2025

Revised Date: 21 June 2025

Accepted Date: 18 August 2025

Please cite this article as: Duan, F., Li, X., Wei, Z., Li, J., Jiang, C., Jiao, C., Zhao, S., Kong, Y., Yan, M., Huang, J., Yang, J., Chen, Y., Bock, R., Zhou, W., Multi-omics analysis reveals distinct responses to light stress in photosynthesis and primary metabolism between maize and rice, *Plant Communications* (2025), doi: https://doi.org/10.1016/j.xplc.2025.101488.

Multi-omics analysis reveals distinct responses to light stress in photosynthesis and primary metabolism between maize and rice

Fengying Duan[1,2,†], Xia Li[1,2,†], Ze Wei[1,†], Jing Li[1], Caifu Jiang[3], Chengzhi Jiao[1], Shanshan Zhao[4], Yu Kong[4], Mengxiao Yan[4], Jirong Huang[5], Jun Yang[4*], Yanmei Chen[3*], Ralph Bock[6*], Wenbin Zhou[1,2,7*]

[1]Institute of Crop Sciences, Chinese Academy of Agricultural Sciences, Beijing 100081, China.

[2]State Key Laboratory of Crop Gene Resources and Breeding, Institute of Crop Sciences, Chinese Academy of Agricultural Sciences, Beijing 100081, China.

[3]State Key Laboratory of Plant Environmental Resilience, College of Biological Sciences, China Agricultural University, Beijing 100193, China.

[4]Shanghai Key Laboratory of Plant Functional Genomics and Resources, Shanghai Chenshan Botanical Garden, Shanghai 201602, China.

[5]Shanghai Key Laboratory of Plant Molecular Sciences, College of Life Sciences, Shanghai Normal University, Shanghai 200234, China.

[6]Max-Planck-Institut für Molekulare Pflanzenphysiologie, Am Mühlenberg 1, D-14476 Potsdam-Golm, Germany.

[7]Research Center of Breeding in Hainan, CAAS.

[†]These authors contributed equally to this work.

[*]Author for correspondence: jyang03@cemps.ac.cn; chenyanmei@cau.edu.cn; rbock@mpimp-golm.mpg.de; zhouwenbin@caas.cn.

The author responsible for distribution of materials integral to the findings presented in this article in accordance with the policy described in the Instructions for Authors is Wenbin Zhou.

SHORT SUMMARY

High light (HL) stress constrains crop yield, with maize (C_4) and rice (C_3) showing distinct adaptations. Multi-omics and physiological analyses reveal rice responds rapidly via photosynthetic and metabolic adjustments, whereas maize relies on cyclic electron flow, non-photochemical quenching, and antioxidant defenses. Key genes (e.g., *ZmPsbS*, *OsbZIP18*) were identified, offering targets for crop improvement.

ABSTRACT

High light (HL) stress is a significant environmental factor limiting crop productivity. Maize (*Zea mays*) and rice (*Oryza sativa*), two key global crops, can both grow under high light intensities, but differ in photosynthetic metabolism, with maize being a C_4 species and rice a C_3 species. However, the molecular mechanisms underlying their responses to HL stress remain poorly understood. To systematically dissect how HL affects growth of maize and rice, we carried out time-resolved multi-omics analyses, examining the transcriptome, translatome, proteome and metabolome in response to HL treatment. Combining this multi-omics approach with physiological analyses, we found that rice exhibits a more rapid response to HL stress than maize, with significant alteration in photosynthetic electron transport, energy dissipation, reactive oxygen species (ROS) accumulation, and primary metabolism. In contrast, the higher tolerance to HL stress of maize is primarily attributed to increased cyclic electron flow (CEF) and non-photochemical quenching (NPQ), elevated sugar and aromatic amino acid accumulation, and enhanced antioxidant activity during a 4-hour HL exposure. Transgenic experiments further validated key regulators of HL tolerance; for instance, knock-out of *OsbZIP18* enhanced HL tolerance in rice, while overexpression of *ZmPsbS* in maize significantly boosted photosynthesis and energy-dependent quenching (qE) after 4 hours HL treatment, underscoring its role in protecting C_4 crops from HL-induced photodamage. Together, these findings offer new insights into the molecular mechanisms of HL stress tolerance in C_4 versus C_3 species, and highlight a set of candidate genes for engineering improved HL tolerance in crops.

Key words: light stress, photoinhibition, non-photochemical quenching, multi-omics, crop

INTRODUCTION

As sessile organisms, plants have evolved remarkable plasticity to adapt to constantly changing environmental conditions. Light, is the most dynamic and variable environmental factor for photoautotrophic organisms, and serves as both energy source and signaling factor that influences numerous cellular processes (Slattery et al., 2018). However, on many days of the life cycle, most plants encounter high light (HL) intensities that exceed their photosynthetic capacity, leading to stress and potential damage to chloroplasts and cells (Karpinski et al., 1999). Such stress disrupts the balance between photosystem activity and carbon fixation, impairing photosynthetic efficiency and reducing crop yields (Li et al., 2020; Long et al., 1994; Yamamoto et al., 2008). In addition, excess excitation energy can result in reactive oxygen species (ROS) accumulation, primarily at photosystem II (PSII) and photosystem I (PSI), accelerating photoinhibition and hindering PSII repair cycles (Asada, 2006; Nishiyama et al., 2006; Raven, 2011).

Plants have evolved various acclimation mechanisms to mitigate to HL stress, including modulation of the photosynthetic machinery at different time scales. For PSII, the dynamic degradation and *de novo* synthesis of the D1 protein is critical for maintaining photosynthetic activity (Edelman and Mattoo, 2008). Non-photochemical quenching (NPQ), which dissipates excess light energy as heat, is a rapid and flexible photoprotection response (Christa et al., 2017). NPQ includes several components, such as energy-dependent quenching (qE) (Krause et al., 1982), photoinhibitory quenching (qI) (Krause, 1988), state transition quenching (qT) (Krause and Weis, 1991), zeaxanthin-dependent quenching (qZ) (Nilkens et al., 2010), sustained antenna quenching (qH) (Brooks et al., 2013; Malnoë et al., 2018) and a blue light-dependent quenching induced by chloroplast movement (qM) (Cazzaniga et al., 2013; Li et al., 2018; Takahashi and Badger, 2011). Among these, qE is the fastest and most significant, driven by the thylakoid lumen acidification, which activates the PSII subunit S (PsbS) and the xanthophyll cycle (Krishnan-Schmieden et al., 2021). Lumen acidification promotes the accumulation of zeaxanthin, a key xanthophyll pigment, further enhancing qE (Bassi and Dall'Osto, 2021; Niyogi et al., 1998); while qI is slowly

induced and relaxed under long term HL exposure caused by the photoinactivation of the D1 protein in the PSII reaction center and zeaxanthin accumulation (Kress and Jahns, 2017; Nilkens *et al.*, 2010). PsbS acts as a sensor of the low lumenal pH generated by photosynthetic electron transfer, triggers conformational changes in the PSII antenna, and ultimately activates NPQ. Increased expression of PsbS and xanthophyll cycle enzymes has been shown to enhance NPQ capacity, photosynthetic efficiency, and crop yields in species like tobacco (*Nicotiana tabacum*) and soybean (*Glycine max*) (De Souza et al., 2022; Kromdijk et al., 2016).

In addition to photoprotection, transcriptional and translational networks regulate the expression of genes encoding photosynthetic proteins, including antenna proteins and core components of the photosynthetic apparatus, enabling efficient acclimation to HL (Huang et al., 2019; Schuster et al., 2020). C_4 plants, such as maize (*Zea mays*), exhibit higher photosynthetic efficiency and HL tolerance than C_3 species like rice (*Oryza sativa*), due to distinct biochemical and anatomical traits. These include spatial separation of (de)carboxylation enzymes in mesophyll and bundle sheath cells, which optimize energy utilization for carbon fixation under stress conditions (Blatke and Brautigam, 2019; von Caemmerer, 2021; Yabiku and Ueno, 2019). While many HL responses are shared between C_3 and C_4 plants, critical differences exist in their regulatory mechanisms, including energy dissipation and acclimation processes.

Maize and rice, as members of the same plant family (Poaceae), provide ideal models for comparative studies of C_3 and C_4 photosynthesis. In this study, we conducted time-resolved multi-omics analyses, integrating transcriptomic, translatomic, proteomic and the metabolomic data, to investigate the HL responses of these two crops over a 4-hour HL treatment. Our results provide insights into NPQ-mediated photosynthetic remodeling, metabolic regulation, and antioxidant defenses, identifying key pathways and regulators of HL tolerance in both species. Genetic validation of several potential regulators highlights promising strategies for improving photosynthetic efficiency and HL tolerance through genetic engineering and crop breeding.

RESULTS

Rice is more sensitive to HL stress than maize in photosynthetic electron transport and energy dissipation

To establish the physiological basis for a multi-omics analysis of HL stress responses, we first evaluated the photosynthetic response of maize and rice to HL intensities. To this end, hydroponically grown seedlings of both species were cultivated under a growth light intensity of 300 μmol photons m^{-2} s^{-1} until the five-leaf stage, followed by exposure to HL intensities of 1800-2000 μmol photons m^{-2} s^{-1} for 4 hours (10 a.m. to 2 p.m.), simulating midday field conditions (Figure S1A). To evaluate the sensitivity of seedlings to HL exposure, we measured the maximum potential quantum efficiency of PSII (F_v/F_m), a proxy of reversible photoprotective down-regulation and/or irreversible photodamage of PSII. F_v/F_m decreased more rapidly in rice than in maize, reaching 0.5 and 0.7, respectively, after 4 h of HL exposure (Figure S1B). This observation indicated distinct photosynthetic responses to HL stress between the two species. Based on these findings, we selected the time points 0 h, 2 h, and 4 h for further physiological and multi-omics analyses.

To explore the mechanistic differences, we analyzed photosynthetic responses in more detail. The dynamic changes of chlorophyll fluorescence were measured, including chlorophyll *a* fluorescence OJIP transient (OJIP transient), photosynthetic electron transport rate (ETR), redox state of the plastoquinone (PQ) pool, maximum photooxidizable fraction of P700 (P_m), F_v/F_m, and non-photochemical quenching (NPQ). HL treatment increased fluorescence in the J-phase of the OJIP curve similarly in both species, indicating comparable plastoquinone A (Q_A) reduction levels in PSII reaction centers (Fig. 1A and Figure S1C). However, fluorescence in the I-phase increased significantly only in rice (Fig. 1A and Figure S1D), suggesting that more pronounced impairment of electron transport from PSII to PSI in rice. Consistently, HL exposure induced opposite changes in ETR(II) and ETR(I) between the species (Figure S2A, B). Accordingly, PQ pool reduction increased significantly in rice during HL treatment, while it remained at a relatively low level for 2 h in maize before increasing at 4 h (Fig. 1B), indicating a more severe disruption of PQ-to-PSI electron transfer in

rice. Similarly, P_m and F_v/F_m significantly decreased in rice after 2 h of HL treatment, but were unaffected in maize until 4 h (Fig. 1C, D). Moreover, the quantum yield of PSII [Y(II)] decreased prominently in rice, but remained unaffected in maize under HL (Figure S2C). While the quantum yield of light-inducible energy dissipation [Y(NPQ)] decreased in both species, the non-regulated energy dissipation [Y(NO)] increased only in rice after 4 h of HL (Figure S2D,E). These data suggest that PSII photodamage occurred in rice but not in maize. We further investigated the NPQ induction and relaxation dynamics in both species. In maize, NPQ was rapidly and highly induced under HL, reaching its maximum within 200 seconds (s) of actinic light (AL) exposure, and relaxing to baseline level within 150 s after AL switch-off. Conversely, rice displayed significantly reduced NPQ after 2 h of HL, and after 4 h, NPQ failed to reach comparable levels as untreated plants (Fig. 1E). These results suggest that NPQ induction and relaxation are severely compromised by HL in rice. Notably, the major NPQ component, qE, decreased strongly in rice after 4 h of HL, while the residual NPQ increased. By contrast, both NPQ components remained stable in maize (Fig. 1F). These data suggest that maize has a stronger ability to dissipate excess absorbed light energy as heat than rice. Gas exchange measurements further showed that the net photosynthetic rate (P_n), the maximum rate of carboxylation (V_{cmax}), and the maximum electron transport rate (J_{max}) decreased significantly in rice, but were only slightly affected in maize following a 4-hour HL treatment (Fig. 1G-I). Taken together, our results demonstrate that maize and rice exhibit distinct photosynthetic responses to HL stress, with maize showing greater resilience in maintaining photosynthetic electron transport and energy dissipation mechanisms under HL conditions.

Multi-omics analysis reveals distinct molecular responses to HL in maize and rice

To elucidate the molecular basis underlying the differential responses of maize and rice to HL, we conducted a comprehensive multi-omics analysis, including transcriptomics, translatomics (ribosome profiling), proteomics and metabolomics (Fig. 2A). In general, both species displayed the strongest responses at the transcriptomic level, followed by translatomics, proteomics and metabolomics (Fig. 2B). Partial least squares projection

to latent structures (PLS) analysis demonstrated that samples from the same time point clustered closely together across all gene expression levels (transcription, translation, and protein accumulation) in both maize and rice (Figure S3A-C). Principal component analysis (PCA) of metabolite profiles revealed distinct metabolic responses to HL in maize and rice, accounting for 59.59% variance along PC1 (Figure S3D). Interestingly, rice samples exhibited higher similarity in PC2 across time points, while maize samples were more dispersed (Figure S3D), suggesting greater temporal variability in maize metabolic responses to HL stress.

Next, we characterized the global response of rice and maize to HL by calculating the number of differentially expressed variables in each omics dataset (Figure S4 and Table S1). After 4 h of HL exposure, 19.18% and 25.92% of genes were transcriptionally upregulated in maize and rice, respectively (Figure S4A). At the translational level, fewer genes were upregulated (9.53% in maize, and 10.77% in rice; Figure S4B and Table S1). Specifically, maize showed 507 and 947 upregulated genes at 2 h and 4 h, , while rice showed 925 and 1681 upregulated genes at these time points. At the proteomic level, maize exhibited a higher proportion of downregulated protein (64.34%) compared to rice (24.21%), corresponding to 585 and 684 downregulated proteins in maize, and 65 and 202 proteins in rice at 2 h and 4 h, respectively (Figure S4C and Table S1). This suggests a faster rate of protein turnover in maize under HL stress. Similarly, a greater accumulation of metabolites was observed in maize than in rice after 2 h and 4 h of HL exposure (Figure S4D).

Coordinated responses across multi-omics levels

To identify regulatory mechanisms underlying the HL response, we searched for genes exhibiting coordinated changes across transcription, translation and protein accumulation levels (Fig. 2C and Dataset S1). This analysis revealed 33 maize genes and 23 rice genes that were significantly altered across all three levels (*adj.* $P < 0.05$). When analyzing co-regulation at two levels, we identified 922 maize genes with coordinated transcriptional and the translational responses, 151 genes with coordinated transcriptional and protein accumulation responses, and 45 with coordinated

translational and protein accumulation responses. Corresponding numbers in rice were 1748, 148 and 27 genes, respectively (Fig. 2C).

Gene ontology (GO) enrichment analysis of genes significantly altered at two or more levels revealed enrichment of terms related to photosynthesis, reactive oxygen species (ROS) response, and temperature stimulus response (FDR < 0.01, $P < 0.05$), indicating that these processes are directly affected by HL stress in both species (Figure S5). Additionally, genes involved in thylakoid membrane formation and photosystem biogenesis were enriched in both maize and rice, consistent with the strong impact of HL on the light reactions of photosynthesis (Figure S5). Interestingly, rice-specific enrichment was observed for genes involved in translation, protein folding, carboxylic acid metabolism, and transmembrane protein transport, suggesting unique molecular adaptations in rice to HL stress (Figure S5B).

Photosynthesis-related genes respond differently to HL in maize and rice

As described above, numerous photosynthesis-related genes exhibited significant responses to HL stress in both maize and rice (Figure S5). Among these, 71 and 42 nucleus-encoded photosynthesis-related genes were differentially regulated in maize and rice, respectively (Fig. 3). Of these, 36 and 28 genes were downregulated at the transcript level in maize and rice, respectively, while only two rice genes (*OsPsbQ3* and *OsPsbS2*) were upregulated after 2 h of HL treatment (Fig. 3B). Closer inspection revealed that maize required 4 h of HL exposure for significant downregulation of *ZmATPF1D2*, *ZmATPF1G*, and several PSI and PSII genes (*ZmPsa*, *ZmLhca*, *ZmPsb* and *ZmLhcb*). In rice, a similar set of genes (*OsNDHB4*, *OsPsa*, *OsLhca*, *OsPsb* and *OsLhcb*) were repressed after only 2 h of HL treatment (Fig. 3A,B,E-G). These findings indicate that photosynthesis-related genes in rice respond more sensitively to HL stress than those in maize.

To further investigate the relationship between translation and protein accumulation during HL stress, we compared ribosome profiling (translatomic) data with differentially expressed proteins (DEPs) datasets. In maize, both translational activity and protein levels of photosynthesis-related genes were simultaneously reduced

at 2 h and 4 h of HL. By contrast, in rice, the abundance of photosynthetic proteins predominantly increased after 2 h of HL, while translational activity remained largely unchanged (Fig. 3A, B, E, H). Collectively, these results suggest that maize primarily downregulates photosynthetic gene expression at all levels in response to HL, whereas rice exhibits more heterogeneous responses across transcriptional, translational, and proteomic levels.

Important roles of primary metabolism during HL stress

To better understand the metabolic adaptations underlying HL-induced changes in photosynthesis, we analyzed primary metabolic pathways—glycolysis, the TCA cycle, and amino acid biosynthesis—by integrating metabolomic data with the transcriptomic, translatomic and proteomic datasets (Fig. 4 and Figure S6). HL stress resulted in increased accumulation of several TCA cycle intermediates, including α-ketoglutarate, fumarate, and malate in both species. Consistently, genes encoding TCA cycle enzymes were highly upregulated—5 in rice and 11 in maize (Figure S6A). However, sugars and glycolytic intermediates (*e.g.*, glucose, fructose, galactose, maltose, and glucose-6-phosphate (G6P)) accumulated more strongly in HL-treated maize plants than in rice. Similarly, the accumulation of amino acid, such as tryptophan, phenylalanine, tyrosine, and tyramine were more pronounced in maize (Fig. 4 and Figure S6B, C). We also detected several metabolites with contrasting accumulation patterns between maize and rice during HL stress. For instance, trehalose accumulated rapidly in maize within 0.5 h of HL exposure, but continuously decreased in rice over 4 h. Correspondingly, genes encoding trehalose-6-phosphate synthase (*TPS*) were upregulated in maize but downregulated in rice (Fig. 4).

Amino acid metabolism also showed differential responses between species. In maize, the levels of aromatic amino acids (AAAs)—phenylalanine, tyrosine, and tryptophan—were significantly elevated, with a strong upregulation of *ZmCMU* (chorismate mutase), a key gene in AAA biosynthetic, after 4 h of HL (Fig. 4). In contrast, both the AAA levels and the expression of the *OsCM* (chorismate mutase)

gene were significantly reduced in rice under HL stress (Fig. 4). Additionally, nitrogen metabolism in maize were enhanced, as evidence by increased glutamine and glutamate, which were key intermediates in the glutamine synthetase/glutamate synthase cycle (GS-GOGAT cycle), as well as proline, putrescine, and spermine accumulation, all of which are common stress markers in plants (Fig. 4 and Figure S6D).

Genes encoding antioxidant defense proteins, including glutathione-S-transferase (GST) and peroxidases (Prx), were significantly altered in both species across multiple omics datasets during HL treatment (Fig. 4 and Figure S6E). Interestingly, nearly 50 % of these genes were transcriptionally upregulated in maize, whereas approximately half were downregulated in rice under HL stress (Fig. 4). Considering the pivotal roles of GST and Prx in mitigating photo-oxidative stress, these findings suggest that the antioxidative defense capacity differs significantly between maize and rice. Although many heat shock proteins (HSPs) and their corresponding mRNAs were detected in our datasets, their abundance did not change significantly in response to HL ($P < 0.05$), indicating that heat stress effects were negligible under the HL treatment conditions (Figure S7).

Taken together, our results demonstrate that maize and rice exhibit distinct responses to HL stress at multiple molecular levels. Enhanced carbohydrate metabolism, nitrogen metabolism, and antioxidative defense systems are tightly associated with the HL response of maize, while rice displays more heterogeneous regulatory changes across transcription, translation, and protein levels.

Efficient remodeling of electron transport and NPQ formation protect maize from photodamage under HL stress

As shown in Fig. 3, multiple genes and proteins whose abundances changed significantly during HL stress were mapped to photosynthetic electron transport processes, including linear electron transfer (LET) and cyclic electron flow (CEF). Notably, a reduction in LET coincided with an increase in CEF. For instance, the expression of CEF genes, including *ZmPetF5/6*, *ZmPnsB1-2, ZmPnsB2* and *ZmPGR5*-

like2/3, was upregulated after 2 h or 4 h of HL, correlating with a 2-3 fold increase in CEF in maize (Fig. 3D,G, Figure S8A). In rice, however, CEF increased 1.5-fold after 2 h of HL but returned to pre-stress level by 4 h. These changes paralleled the expression patterns of *OsNDHB4*, *OsPGR5*, and *OsPGR5 like* transcripts, and the OsNDHM protein (Fig. 3G and Figure S8A). Considering the pivotal role of PsbA (D1) protein in the repair of photodamaged PSII, we further examined the expression level of this protein by western blot analysis. Our results showed that D1 protein levels decreased more slowly in maize than in rice under HL (Figure S8B), highlighting the essential role of electron transport and PSII repair in mitigating photodamage in maize.

Despite the general downregulation of photosynthesis-related genes under HL stress, *PsbS* and *PetF* were upregulated in both maize and rice (Fig. 3B,D,I). The increased expression of *PsbS* is consistent with the physiological acclimations of maize and rice to HL, as the PsbS protein and the xanthophyll cycle are major regulators of NPQ. In maize, *ZmPsbS* were highly induced after 4 h of HL, while in rice, *OsPsbS1* and *OsPsbS2* were significantly induced after 2 h (Fig. 3I). Among the three key xanthophyll cycle enzymes—β-carotene hydroxylase (Chs; *ZmHYD4*, *ZmHYD5*, *OsBCH1*, *OsHYD3*), violaxanthin de-epoxidase (VDE; *ZmVDE1*, *OsVDE*), and zeaxanthin epoxidase (ZEP; *ZmZEP1*, *ZmZEP2*, *OsZEP1*)—*Chs* and *VDE* were transcriptionally upregulated in maize but remained unaffected in rice. Conversely, *ZEP* was significantly upregulated only in rice (Figure S8C-F). These results suggest that increased expression of xanthophyll cycle enzymes contributes to HL tolerance in maize by maintaining high NPQ level.

To further examine the role of NPQ in the differential HL responses, we generated *PsbS* knockout (KO) mutants (*psbs*) and overexpression (OE) lines in maize. Under normal light condition, *ZmPsbS*-OE plants displayed enhanced growth characteristics, including longer roots, increased plant height, and higher biomass compared to wild-type (WT) plants, while the *ZmPsbS*-KO plants exhibited opposite phenotypes (Fig. 5A and Figure S9A). Under HL stress, the F_v/F_m values remained stable in *ZmPsbS*-OE plants but declined significantly in *ZmPsbS*-KO plants after 2 h and 4 h of HL (Fig. 5B). This suggests that *PsbS* plays a critical role in HL tolerance, as reduced F_v/F_m values

in HL-treated *psbs* mutants likely reflects impaired photoprotection. Other photosynthesis-related parameters, such as photosynthetic rate, stomatal conductance, and transpiration rate, followed similar trends, except for intercellular CO_2 concentration (Fig. 5C and Figure S9B). Interestingly, maize *psbs* mutants displayed a pronounced increase in the I phase of the OJIP curve compared to the WT, mimicking the HL response observed in rice (Fig. 5D and Figure S1C-D). In contrast, maize *PsbS*-OE lines showed no significant alterations in the J or I phases during HL treatment (Fig. 5D), indicating that *PsbS* positively regulates photoprotection. Consistently, both ETR(II) and ETR(I) decreased in *psbs* mutants and increased in OE lines after 4 h of HL (Figure S9C,D). Furthermore, analyses of NPQ induction and relaxation revealed that the NPQ, particularly its qE component, declined rapidly in *psbs* mutants under HL stress but increased in OE lines and WT plants (Fig. 5E). Taken together, these results demonstrate that NPQ formation is essential for the HL response in maize, and elevated *ZmPsbS* expression enhances qE, thereby improving plant tolerance to HL stress.

Integrated correlation networks identify key components in HL-responsive regulation of gene expression in maize and rice

To identify candidate genes responsible for HL tolerance and to elucidate their interrelationships, we applied machine learning methods to construct gene correlation networks using our multi-omics datasets. Four distinct machine learning algorithms were employed to determine the weight value of the variables (i.e., genes, proteins) that respond to HL. To this end, non-redundant genes from the top 10,000 interactions were clustered based on the weight values using the Infomap method (Figure S10). The network analysis revealed that numerous transcription factors (TFs) and photosynthesis-related genes act as hub nodes in both maize and rice. For example, the maize network contains 20 TF hub genes representing diverse families, including DOF, CO-like, AP2-EREBP, bHLH, NAC, MYB, TCP, bZIP, WRKY, ERF, and NF-Y TFs. The rice network contains 9 TF hub genes, including GRAS, zinc finger, MYB, bZIP, MAD, and NF-Y TFs. In addition, a greater number of photosynthesis-related hub genes were identified in maize, while only a few key genes were found in rice such as

OsPsbS2 (*Os04g0690800*), chlorophyll a/b binding proteins (*Os11g0242800*，*Os01g0720500*，*Os07g0577600*), fructose-bisphosphate aldolase (*Os11g0171300*), and malate dehydrogenase (*Os08g0434300*) (Dataset S3).

In maize, the analysis revealed seven gene modules integrated into the correlation networks, with three biological processes—photosynthesis, oxidative stress, and metabolic pathways—being highly enriched (Figure S10A and Dataset S2). Quantitative analysis identified 424 node genes that exhibited significant changes during the 4 h HL stress period (Dataset S3). These changes were primarily observed at the transcriptional level (269 out of 450 genes) and in protein accumulation (184 out of 450 proteins). Among these node genes, 14 displayed simultaneous decreases at the transcriptional, translational, and protein accumulation levels. These included genes involved in photosynthesis, oxidative stress responses, and central metabolism, such as *ZmPsb27* (*Zm00001d029049*), *ZmPsaD1* (*Zm00001d013039*), *ZmPsaE1* (*Zm00001d005446*), *peroxidase* 5 (*ZmPrx5, Zm00001d037550*), an *auxin-repressed protein* gene (*Zm00001d029102*), and *PDK regulatory protein1* (*ZmPDRP1*, *Zm00001d006520*). Notably, genes encoding fructose-bisphosphate aldolase (*Zm00001d023559*) and DNA-directed RNA polymerase (*Zm00001d019553*) were identified as key nodes connected with multiple modules. Moreover, *ZmPsaE* genes acted as central hubs in the module associated with photosynthetic electron transport and PSII repair, while *ZmPsaD1* was part of a module linked to chlorophyll biosynthesis and PSI light harvesting (Figure S10A), implying that these genes may play regulatory roles in the HL response in maize. Overall, these results highlight the close linkage and extensive reprogramming of photosynthesis and carbon metabolism during HL stress.

In rice, the analysis identified six modules within the gene correlation networks. Similar to maize, these modules were functionally associated with photosynthesis, oxidative stress responses, and metabolism (Figure S10B and Dataset S2). Quantitative analysis revealed significant changes in 297 node genes, with 251 showing transcriptional changes and 113 exhibiting alterations at the translational level. Interestingly, only one gene (*Os01g0303000*) displayed changes across all three levels

(Dataset S3). This gene encodes the regulator protein CP12, which is involved in thioredoxin-mediated regulation of the Calvin-Benson cycle in response to light (López-Calcagno et al., 2017). Network analysis demonstrated that genes involved in photosynthesis and metabolic processes clustered within the same modules, reflecting their interconnected roles in HL acclimation. In addition, genes related to the GO terms 'response to hydrogen peroxide' and 'protein complex oligomerization' clustered together (Figure S10B), suggesting a potential interplay between oxidative stress and protein complex formation under HL stress. Importantly, the correlation network analysis identified three transcription factors—*OsbZIP18* (*Os02g0203000*), *OsARP1* (*Os11g0671000*), and *OsHAP5C* (*Os03g0251350*)—as central hubs connecting different modules (Figure S10B). This finding suggests that these transcription factors may play pivotal roles in regulating HL responses in rice.

The OsbZIP18 transcription factor regulates HL tolerance in rice

Pronounce changes in gene expression and physiological processes occurred 2 h earlier in rice than in maize during HL stress, suggesting that the two crops have evolved distinct regulatory mechanisms to cope with HL challenges. Given the crucial role of transcription factors (TFs) in orchestrating gene expression under stress, we compared the expression patterns of HL-responsive TF genes in maize and rice (Dataset S4). A total of 161 maize and 119 rice TF genes responded significantly to HL treatment. These included genes encoding AP2-EREBP, BTF, bHLH, bZIP, ERF, GATA and MYB TFs, indicating conserved roles in HL-induced gene regulation across both crops (Dataset S4). Interestingly, while eight *bZIP* genes were significantly upregulated in maize after 4 h of HL exposure, only one rice gene, *Os02g0203000/OsbZIP18*, was induced after 2 h and peaked after 4 h of HL. Remarkably, *OsbZIP18* was identified as the central hub gene in our correlation network analysis. Its expression level negatively correlated with the reductions in F_v/F_m and the photosynthetic rate in rice (Dataset S3 and Fig. 1D, E).

To determine whether *OsbZIP18* contribute to HL tolerance, we generated two CRISPR-Cas9 KO mutants, referred to as *Osbzip18*-KO1 and *Osbzip18*-KO2 (verified

414 by PCR and sequencing) (Fig. 6A). The physiological responses of these knockout lines
415 to HL treatment were subsequently compared to those of the WT and the *OsbZIP18*
416 overexpression plants (OE1; Fig. 6B). The OE1 line was generated in the Zhonghua 11
417 (ZH11) background, while the knockout (KO) lines were in the Nipponbare (NIP)
418 background. Consequently, physiological data from the OE and KO lines were
419 compared with those from their respective wild-type (WT) control. As shown in Fig. 6,
420 both F_v/F_m and P_n progressively declined in wild-type plants with extended HL
421 exposure (Fig. 6C,D). Notably, the KO lines displayed a slower reduction in these
422 parameters than the WT (NIP), indicating increased tolerance to HL. By contrast, the
423 OE1 line exhibited a significantly faster and more pronounced decrease in F_v/F_m and
424 P_n, with the levels at 2 h HL being comparable to those of ZH11 at 4 h HL (Fig. 6C,D),
425 suggesting enhanced sensitivity to HL stress. Similar trends were observed in
426 transpiration rate, stomatal conductance, and intercellular CO_2 concentration (Figure
427 S11A-C).

428 Further assessment of non-photochemical quenching (NPQ) and its components
429 revealed distinct responses. While total NPQ in KO lines decreased at a similar rate as
430 in the WT, the qE component declined more slowly, with a significant reduction
431 observed only after 4 h HL. By contrast, OE lines exhibited a more rapid decrease in
432 NPQ and qE, with significant reductions evident by 2 h HL (Fig. 6E, Fig. S11D). These
433 results collectively demonstrate that *OsbZIP18* dosage significantly influences HL
434 tolerance, supporting its regulatory role in the HL response.

435 To further investigate the regulatory function of OsbZIP18, we performed RNA-
436 seq analysis of WT, KO, and OE lines under HL conditions. Differential expression (4
437 h HL vs. 0 h) and clustering analyses identified a group of genes (Cluster 9 in Figure
438 S12) that were downregulated in WT and/or OE lines, but remained stable in KO lines.
439 Gene Ontology (GO) enrichment analysis revealed that these genes were involved in
440 photosynthesis, NPQ-related processes, oxidative stress response, and nitrate transport
441 (Figure S12). Additionally, analysis of DEGs (*adj.* $P < 0.05$) demonstrated that key
442 genes related to light harvesting (Lhca/b), NPQ, PSII assembly, and oxidative stress
443 exhibited distinct expression patterns across WT, KO, and OE lines following HL

treatment (Fig. 6F). These findings suggest that OsbZIP18 modulates a set of stress-responsive and photosynthesis-related genes, thereby contributing to the regulation of the physiological adaptations to HL stress in rice.

DISCUSSION

Light stress at midday, particularly in the summer season, is a common adverse condition that negatively affects plant performance in the field. Exposing plants acclimated to normal growth condition (300 μmol photons m^{-2} s^{-1}) to midday light intensity (1800 μmol photons m^{-2} s^{-1}) is a relevant experimental approach for breeding or engineering HL tolerant field grown crops. Although significant progress has been made in understanding the molecular mechanisms underlying plant tolerance to HL, the master regulators determining HL tolerance remain largely unidentified. Here, we applied a systems biology approach to unravel the physiological and molecular responses to HL stress and identify the underlying mechanisms in two model crops with distinct photosynthetic metabolism: the C_4 plant maize and the C_3 plant rice. While transcriptomic responses to HL stress were extensive (with 10,897 DEGs in maize and 10,863 in rice), only 16.4% (maize) and 8.5% (rice) of these genes showed concordant changes at the protein level. Although transcriptional and translational responses were broadly aligned, mRNA-protein correlations were weaker, consistent with prior studies in *Arabidopsis* (Liang et al., 2016; Li et al., 2022). These results underscore the role of post-transcriptional mechanisms, including translational regulation and protein turnover, in shaping stress responses.

Additionally, we identified conserved and specific responses to HL stress in the two crops. Physiological analyzes revealed that photosynthesis was affected by HL in both species; however, F_v/F_m, NPQ, and the photosynthetic rate decreased more rapidly in rice than in maize (Fig. 7). This observation is consistent with the higher sensitivity of rice to HL stress. The multi-omics analysis further supported these findings, showing early transcriptional responses (within 2 h) in both crops. Genes involved in photosynthesis and chlorophyll biosynthesis were downregulated, while ROS-

responsive genes were induced. At the translational level, processes such as protein folding/unfolding and ROS responses were among the most affected. These changes were accompanied by a pronounced reduction in the abundance of photosynthetic complex components (*e.g.,* PSI, PSII), leading to reduced light harvesting and electron transport (Fig. 3, Fig. 7 and Figure S2). The rapid transcriptional and translational regulation observed in rice within 2 h of HL stress suggests that the ROS burst triggered by HL exposure quickly represses photosynthetic processes (Mittler et al., 2022). In contrast, maize largely maintained homeostasis during this period, indication a more robust tolerance mechanism. Interestingly, while photosynthesis-related genes were transcriptionally downregulated in HL-treated rice, their corresponding protein levels increased. This discrepancy could reflect HL-induced structural rearrangements of thylakoid membrane protein complexes (Kim et al., 2020), or the delayed effect of *de novo* protein synthesis. Together, these findings indicate that the C_3 plant rice experiences HL stress earlier and initiates a faster response than the C_4 plant maize.

It is well established that plants mitigate HL-induced photodamage by reducing light absorption, quenching excess light energy, repairing damaged PSII, and scavenging ROS (Shi et al., 2022). Our study disclosed several photoprotective pathways that were differentially regulated in maize and rice under the same HL intensity (300 μmol photons m^{-2} s^{-1} to 1800 μmol photons m^{-2} s^{-1}). In maize, the abundance of the D1 protein increased (Figure S8B), suggesting efficient PSII repair. Additionally, CEF around PSI was elevated in maize under HL (Figure S8A), likely providing extra ATP for the CO_2 concentration mechanism (CCM) operating in C_4 photosynthesis (Ishikawa et al., 2016; Munekage and Taniguchi, 2016). Maize also exhibited upregulated expression of *PsbS*, *Chs* and *VDE* genes, potentially increasing the zeaxanthin pool size and enhancing NPQ (Figure S8D-F). In contrast, both *Chs* and *VDE* were downregulated in rice. This finding highlights the prominent role of NPQ as a photoprotective mechanism in the C_4 plant, which has not been sufficiently appreciated for a long time. A previous study in the C_4 model plant *Setaria viridis* detected transcriptional changes in *PsbS* gene expression after HL treatment, suggesting that the upregulation of NPQ and *PsbS* gene participate in photoprotection in C_4 plants

(Anderson et al., 2021). However, the functional validation of PsbS in C_4 crops, especially maize, has not been reported. Our transgenic analyses with both *ZmPsbS*-OE and *psbs* mutant revealed that *ZmPsbS* contributes substantially to NPQ induction (Fig. 5 and Figure S9), which is crucial to sustain the photosynthetic capacity in maize upon exposure to HL. Thus, genetic manipulation of key regulators involved in NPQ formation provides a promising and efficient strategy to improve photosynthesis and agricultural productivity in C_4 crops.

Due to their sessile lifestyle, plants depend on metabolic adaptations to achieve stress resilience. In this study, metabolomic analyses revealed significant differences in primary metabolism between maize and rice during HL stress. Maize accumulated higher levels of sugars and sugar conjugates, reflecting its ability to sustain efficient carbon assimilation under HL (Fig. 4 and Figure S6B). Trehalose levels was particularly elevated in maize, suggesting its role as an osmo-protectant and membrane stabilizer to maintain cellular integrity under the stressful conditions (Fernandez et al., 2010). Genetic manipulation or chemical intervention in trehalose metabolism can improve crop yield under stress (Griffiths et al., 2016; Kretzschmar et al., 2015; Paul et al., 2018). Our data reported here suggest that engineering trehalose biosynthesis could be a useful strategy to enhance HL tolerance in crops.

Our study also provided ample evidence for HL stress disturbing the balance of ROS generation and detoxification (Fig. 4 and Figure S6E). To examine changes in ROS levels, we used DAB staining to detect H_2O_2, and NBT staining to measure superoxide (O_2^-) in maize and rice leaves after HL exposure. The DAB staining showed increased H_2O_2 accumulation after 2–4 h of HL treatment in both plant species (Figure S13A), while the NBT staining revealed significantly higher O_2^- accumulation in rice, particularly after 2 h of treatment (Figure S13B). We also analyzed the expression patterns of oxidative stress-related genes. In rice, *SOD*, *POX*, *GSR*, and *GPX* genes were significantly upregulated starting at 2 h post-treatment, whereas in maize, only SOD and *GLPX* were upregulated at 4 h, and *POX/GSR* remained largely unchanged (Figure S14A–D). Interestingly, *CAT* genes were upregulated in rice but downregulated in maize (Figure S14E), further supporting the conclusion that rice suffers more severe

ROS stress under HL. Additionally, maize showed increased expression of *ZmGAD1* and *ZmGLN2*, genes associated with the glutathione (*GSH*) and antioxidant defense systems. It is well established that the GSH/ glutathione disulfide (GSSG) redox system participates in the maintenance of redox homeostasis in plants (Szalai et al., 2009). Whether the higher capacity of maize to maintain redox homeostasis or the redox state of the GSH pool in maize differs from that in rice in response to HL, will need further investigation.

Our transcriptomic and metabolomic datasets provided evidence of accelerated TCA cycle activity under HL stress in both maize and rice (Fig. 4 and Figure S6A). This finding implies that the additional ATP and carbon skeletons generated by the TCA cycle are critical for plants to cope with HL stress (Zhang and Fernie, 2018). In C_4 plants, RuBisCO functions almost exclusively as a carboxylase due to suppression of its oxygenase activity (and the resulting photorespiratory pathway) by the CCM, which elevates CO_2 levels around RuBisCO in the bundle sheath cells. This mechanism is particularly advantageous under harsh conditions such as light or drought stress, where stomatal closure leads to CO_2 limitation and reduces photosynthetic efficiency (Moroney et al., 2013). We further investigated photorespiration-related metabolism and found pronounced species-specific differences. Photorespiration is widely regarded as an energetically costly and inefficient pathway, especially under stress conditions. Notably, the glycine-to-serine ratio, a well-established indicator of photorespiratory flux, increased significantly in rice after 0.5 hours of HL treatment, while it remained very low and largely unchanged in maize (Figure S15). These results demonstrate that rice displays greater sensitivity to HL stress and a lower efficiency of energy utilization than maize. Consequently, it is reasonable to assume that maize, as a C_4 plant, possesses a greater capacity to maintain the homeostasis of its primary metabolism, including sugar and amino acid metabolism, compared to the C_3 plant rice.

Our systems approach and correlation network analysis identified the transcription factor OsbZIP18 as a potential master regulator of HL responses in rice. Transgenic experiments confirmed the critical role of this transcription factor, as knockout mutants (*Osbzip18*-KO) exhibited improved HL tolerance (Fig. 6 and Figure S11). A homolog

of *OsbZIP18* in *Arabidopsis*, *ELONGATED HYPOCOTYL 5* (*HY5*), is a key regulator of light signaling and a wide range of physiological processes, including photomorphogenesis, root growth, nutrient acquisition, and abiotic stress response. In tomato (*Solanum lycopersicum*), HY5 directly activates *PGR5* and *VDE*, which are critical for photoprotection (Jiang et al., 2020). Previous studies on rice have shown *OsbZIP18* as a positive regulator of branched-chain amino acid biosynthesis and a negative regulator of UV-B tolerance (Sun et al., 2022). Two other homologs of *AtHY5* in rice, *OsbZIP1* (Bhatnagar et al., 2023) and *OsbZIP48* (Burman et al., 2018), were reported to mediate seedling photomorphogenesis via alternative splicing and modulation of GA biosynthesis. The new function uncovered in this study highlights *OsbZIP18* as a promising target for genetic engineering to improve photosynthesis under adverse environmental conditions.

In conclusion, our work has revealed novel processes and players in maize and rice that had not previously been implicated in HL tolerance, including several genes with unknown functions that merit future investigation. The study highlights the value of integrating physiological analyses with multi-omics datasets and transgenic experiments to identify master regulators of stress responses. Differences in the response between the C_4 plant maize and the C_3 plant rice were particularly evident in the early phase after the onset of HL stress, in line with the higher sensitivity of rice to the stress. Our findings provide a rich resource of genome-wide expression data and reveal both conserved and species-specific aspects of HL response in maize and rice. These insights can guide future efforts to improve photosynthesis and crop productivity under challenging environmental conditions and in the face of climate change.

METHODS

Plant growth conditions and sample collection

Rice (*Oryza sativa* L. japonica cv. Nipponbare) and maize (*Zea mays* L. cv. B73) were grown hydroponically in a growth chamber (27 °C/20 °C, 16 h/8 h day/night, 300 µmol photons m^{-2} s^{-1}). Rice nutrient solution was based on Yoshida et al. (1976), and maize

on a modified Hoagland solution. The pH was adjusted to 5.9, refreshed every 3 days, and aerated. Seedlings at the five-leaf developmental stage were subjected to 1800 μmol photons m^{-2} s^{-1} high light (HL) for 0 h, 2 h, or 4 h using LED light (model BLS4060, designed by the Plantsystem, HL treatment was applied from 10 a.m.–2 p.m.), Fans were arranged around the LED light source to support heat dissipation, and the room temperature was kept at approximately 25 °C by an air-conditioning system.

As shown in Figure S1A, only the leaf segments that received maximum light exposure were sampled and used for multi-omics analyses or physiological measurements. For RNA extraction, ribosome profiling, and proteomic analysis, leaf segments were rapidly excised and flash-frozen in liquid nitrogen. All experiments were conducted with 3–4 independent biological replicates per treatment group. For the multi-omics analyses, a pooled-sample strategy was employed, in which multiple individual leaves were combined into a single biological replicate to minimize technical variability and enhance data robustness.

Gas exchange measurements

Gas exchange parameters were measured using a LI-6400XT instrument (LI-COR) under 1800 μmol photons m^{-2} s^{-1} PPFD, 500–600 μmol mol^{-1} CO_2, and the leaf temperature was kept between 28 and 30 °C. For the CO_2-response curves (A-C_i), the PPFD was set to 1800 μmol photons m^{-2} s^{-1}, and the CO_2 concentration started at 400 μmol mol^{-1}. Once the steady state had been reached, the CO_2 concentration was decreased stepwise to 50 μmol mol^{-1}, and then gradually increased to 1500 μmol mol^{-1}, for a total of 12 CO_2 concentration values (Long and Bernacchi, 2003). The maximum carboxylation velocity (V_{cmax}) and the maximum electron transport rate (J_{max}) were calculated by fitting the mechanistic model of CO_2 assimilation from the A-Ci curve. V_{cmax} and J_{max} were normalized to values at 25 °C, according to previously described equations (Bernacchi et al., 2001; McMurtrie and Wang, 1993). Four biological replicates were analyzed.

Chlorophyll fluorescence and P700 absorption measurements

F_v/F_m and OJIP fluorescence transients were measured using a FluorPen FP100 after 30 min dark adaptation. NPQ, NPQ components, PSII/PSI fluorescence, and P700 absorption were measured with a DUAL-PAM-100 following standard protocols. Quantum yields (Y(II), Y(NPQ), Y(NO)) and cyclic electron flow (CEF) were calculated. The redox state of PQ pools was determined via OJIP transients with far-red pre-illumination. See the supplemental information for details.

Ribosome profiling and RNA-seq analysis

Ribosomes were extracted from ~2.5 g leaf tissue using polysome extraction buffer, purified via sucrose cushion centrifugation, and subjected to RNase I digestion. Ribosome-protected fragments and RNA were isolated, sequenced, and analyzed. FASTQ files were mapped to maize (*Zea mays* B73_RefGen_v4.41) and rice (*Oryza sativa* IRGSP-1.0) genomes using HISAT2 and processed with Cufflinks. Differential expression was determined using t-tests ($P < 0.05$). See the supplemental information for details.

Protein extraction and peptide identification by mass spectrometry

Proteins were extracted using phenol-based methods, digested with trypsin, and analyzed via Orbitrap Fusion mass spectrometry. Peptides were separated using reverse-phase chromatography, and data were processed with MaxQuant (FDR < 0.01). See the supplemental information for details.

Metabolite profiling

Leaf samples were harvested before and after HL (0.5–4 h) and extracted in methanol with ribitol as an internal standard. Polar metabolites were derivatized with MSTFA and analyzed using GC/Q-TOF-MS. Data were normalized to ribitol and sample weight, then $\log_2$-transformed for PCA. See the supplemental information for details.

Bioinformatic analysis

644 Ribosome isolation and profiling followed previous protocols (Li et al., 2013; Ingolia
645 et al., 2012). Total RNA was extracted, and libraries were sequenced using Illumina
646 HiSeq. Data were mapped to *Zea mays* (B73_RefGen_v4.41) and *Oryza sativa*
647 (IRGSP-1.0) reference genomes, and statistical analysis identified differentially
648 expressed genes/proteins. See the supplemental information for details.

649 **Correlation network analysis**

650 Machine learning methods were employed to determine the weight values of
651 genes/proteins in response to high-light (HL) treatment, using the top 50 differentially
652 expressed genes and unchanged genes as training datasets. The pairwise Spearman
653 correlation coefficients between genes/proteins were calculated using transcriptome,
654 ribosome profiling, and proteome datasets to construct networks, with each interaction
655 weighted based on gene weights and correlation coefficients. The resulting networks
656 were analyzed for community structure and enriched biological processes using tools
657 like igraph and KOBAS. See the supplemental information for details.

658 **Transgenic constructs**

659 Stable transgenic materials generated in this study included the maize *psbs* mutant,
660 maize *PsbS* overexpression lines (*ZmPsbS*-OE), and rice knockout lines of the
661 *OsbZIP18* (*Os02g0203000*) gene. The maize mutant and overexpression lines were
662 generated in the B73 genetic background. The *psbs* mutant was generated by employing
663 the CRISPR/Cas9 knockout method with vector pXUE411C, in which gRNA
664 expression is driven by the OsU3p promoter (targeting locus *Zm00001d042697*) (Xing
665 et al., 2014). Homozygous knockout lines were selected by PCR amplification followed
666 by amplicon sequencing. The *ZmPsbS*-OE line was generated using the over-expression
667 vector pBCXUN, in which transgene expression is driven by the maize UBI promoter
668 (Chen et al., 2009), and homozygous plants were obtained by herbicide selection. Rice
669 knockout lines of the *OsbZIP18* (*Os02g0203000*) gene were generated in the
670 Nipponbare genetic background. CRISPR/Cas9 genome editing was employed to create

the knockout lines using a construct generated with the psgR-Cas9-Os vector backbone (Mao et al., 2013). Two knockout lines of the *OsbZIP18* gene (KO1, KO2) were selected by PCR and sequencing, and used for phenotypic analyses under HL conditions.

Statistical analysis

In all experiments, at least 3 independent replicates were used for data collection and analysis. Data were analyzed using Sigmaplot. Error bars indicate ± standard deviation (SD; $n \geq 3$) according to Tukey's multiple tests at the $P < 0.05$ level. Significant differences are indicated by different letters. n.s. means not significant.

DATA AND CODE AVAILABILITY

- All data are included in the article and/or supplemental information.
- Raw sequence data generated in this study have been deposited in the NCBI BioProject database under accession number PRJNA1072331 and PRJNA1293730 for RNA-seq, and PRJNA1072284 for Ribosome profiling data. The mass spectrometry proteomics data have been deposited to the ProteomeXchange Consortium via the PRIDE partner repository with the dataset identifier PXD049035.

FUNDING

This research was supported by grants from the Key Program of National Natural Science Foundation of China (32330079), Nanfan Special Project, CAAS (YBXM2321), the General Program of National Natural Science Foundation of China (32372027, 32472040, 32170409), the Innovation Program of the Chinese Academy of Agricultural Sciences, the National Key Research and Development Program of China (2023YFE0109500) and Biological Breeding-National Science and Technology Major Project (2023ZD04072).

AUTHOR CONTRIBUTIONS

W.Z., Y.C., and J.Y. designed the research; F.D., X.L., and Z.W. performed most of the experiments; C.F.J. generated the CRISPR/Cas9 knockout and the overexpression lines in maize; J.L. and Y.C. performed the proteomic analyses; C.Z.J. and W.X. performed bioinformatic analyses; S.S.Z and Y.K. performed the metabolomic analyses; all authors participated in data analysis. F.D., X.L., and W.Z. prepared the first draft of the manuscript, which was subsequently revised and edited by R.B. and J.H. All other authors discussed and commented on the manuscript.

ACKNOWLEDGMENTS

We are grateful to Dr. Cheng Jin and Jie Luo from Hainan University for providing rice *OsbZIP18* overexpression material (OE1). We thank Dr. Junjie Fu, Dr. Zefu Lu, and Dr. Hongwei Zhang from the Institute of Crop Sciences, CAAS, for constructive suggestions on data analysis. We thank Dr. Yijing Zhang from Fudan University for providing valuable comments on the manuscript, and Wei Xu from Smartgenomics Technology Institute, Tianjin, for assisting with correlation network analysis.

FIGURE LEGENDS

Figure 1. Physiological response to HL stress in maize and rice. **(A)** OJIP chlorophyll fluorescence transient curves measured in maize (left panel) and rice (right panel) leaves. **(B)** Fraction of reduced plastoquinone (PQ) in maize and rice leaves as determined by fluorescence measurements with a DUAL-PAM-100 instrument (see Methods for calculation). **(C)** Oxidizable fraction of P700 in maize and rice leaves shown as relative P_m (relative to the initial values at 0 h; see Methods). **(D)** Maximum quantum yields of PSII (F_v/F_m) measured in maize and rice leaves upon HL treatment. **(E)** Influence of HL stress on NPQ induction and relaxation in maize (left) and rice (right). **(F)** Percentages of NPQ components in maize (left) and rice (right). Differences in qE (lower part, green color) and residual NPQ (R, upper part, yellow color) between time points in maize and rice were analyzed by one-way ANOVA. **(G)** Photosynthetic rates in maize and rice leaves upon HL treatment. **(H)** Changes in the maximum rate of Rubisco-mediated carboxylation (V_{cmax}) upon HL treatment. **(I)** Changes in the maximum electron transport rate (J_{max}) induced by HL treatment. V_{cmax} and J_{max} were normalized to values at 25 °C. Significant differences at the $P < 0.05$ level are indicated by different letters. $n = 3$. n.s. = not significant.

Figure 2. Overview of high-light (HL) stress-induced changes at the transcriptomics, translatomic, proteomic and metabolomic levels in maize and rice. **(A)** Experimental setup for sampling of maize (M) and rice (R) plants under HL treatment. Leaf samples were taken at the indicated time points and used for transcriptome, ribosome profiling, proteome and metabolome analyses. **(B)** Overall changes in the transcriptome, translatome, proteome and metabolome in maize (upper row) and rice (lower row) in response to HL. **(C)** Venn diagrams illustrating the overlap of differentially expressed genes and proteins at the transcriptional, translational and protein accumulation levels in maize and rice upon HL treatment for 2 or 4 h. Data for the two time points were combined. Changed no. refers to the number of genes or metabolites changed (both positively or negatively) compared with 0h sample.

740 **Figure 3.** Quantitative analysis of the expression of photosynthesis-related genes that
741 respond to HL stress in maize and rice. The heatmap shows the expression patterns of
742 photosynthesis-related genes at the level of mRNA accumulation (RNA), ribosome
743 footprint abundance (RFP) and protein accumulations (Prot). **(A-H)** Nucleus-encoded
744 photosynthetic DEGs (differentially expressed genes) related to LHCII in PSII **(A)**,
745 photosystem II **(B)**, Cytb6f complex **(C)**, electron transport **(D)**, photosystem I **(E)**,
746 LHCI in PSI **(F)**, CEF **(G)** and ATPase **(H)** in maize and rice, respectively. Gene names
747 are given at the left. The values represent $\log_2$ fold-changes ($\log_2$FC). The colors of the
748 boxes indicate upregulation (red) or downregulation (blue) at the $P < 0.05$ level. White
749 boxes denote no significant change, grey boxes indicate lack of data. **(I)** Relative
750 expression of up-regulated genes in both maize and rice at the transcriptional level after
751 2 or 4 hours of HL treatment. Colors in the schematic of the photosynthetic complexes
752 at the top indicate common (blue, down-regulated; red, up-regulated) or different
753 changes (yellow) in maize and rice on transcriptional level.
754
755 **Figure 4.** Changes in central carbon metabolism over time during HL stress in maize
756 and rice. Changes in metabolites, transcripts, ribosome footprints and protein
757 accumulation are shown as heatmaps and are presented as the average of $\log_2$FC during
758 HL treatment (0.5 h, 1 h, 2 h and 4 h for metabolites; 2 h and 4 h for transcripts,
759 ribosome footprints and proteins) compared to the control (before high light).
760 Red/purple and blue/green colors indicate higher and lower $\log_2$FC values, respectively.
761 The upper sets are the rice genes/proteins, the lower sets present the maize
762 genes/proteins.
763
764 **Figure 5.** Comparison of physiological responses in wild-type maize plants (WT), the
765 *psbs* knockout mutant, and *PsbS* over-expression (OE) lines during HL stress. **(A)**
766 Growth phenotypes of plant lines analyzed. **(B-C)** The maximum quantum yields of
767 PSII (F_v/F_m) **(B)** and the photosynthetic rates **(C)** were measured in the wild type, the
768 *psbs* mutant and the *PsbS*-OE lines after 0-4 hours of HL exposure. Significant
769 differences are indicated by different letters at the $P < 0.05$ level (n=3-4). **(D)** The OJIP

chlorophyll fluorescence transients and the changes in fluorescence intensities V_j (at 2 ms) and V_i (at 30 ms) in response to HL treatment were compared between the three genotypes. Significant differences are indicated by different letters ($P < 0.05$). n.s. means no significant difference. Data were analyzed by one-way ANOVA. **(E)** NPQ induction and relaxation (left), and contributions of the two major NPQ components (right). Differences in qE (lower part, green color) and residual NPQ (R) (upper part, yellow color) were analyzed by one-way ANOVA. Significant differences at the $P < 0.05$ level are indicated by different letters (n = 3-4).

Figure 6. Photosynthetic responses to high-light stress in *OsbZIP18* knockout and overexpression lines, and associated differential gene expression. Changes in photosynthesis-related parameters and NPQ upon HL treatment in wild-type rice plants (WT) and *OsbZIP18* KO lines. **(A)** Frame shift mutations induced by genome editing in the two *OsbZIP18* knockout lines. **(B)** Expression of the *OsbZIP18* gene in overexpression line OE1 compared to the wild type (WT). **(C-E)** HL-induced changes in the F_v/F_m ratio **(C)**, photosynthetic rates **(D)**, and NPQ components **(E)** in WT, *OsbZIP18* knockout lines and *OsbZIP18* OE1 line upon HL treatment. Significant differences are indicated by different letters ($P < 0.05$). Data were analyzed by one-way ANOVA (n = 3-4). qE indicates energy-dependent quenching; R indicates the residual NPQ. **(F)** Differentially expressed genes (DEGs) at 4h HL vs. 0 h (*adj.* $P < 0.05$) in WT, KO lines and OE1 plants.

Figure 7. Model of the responses to HL stress in maize and rice at different levels. Significant changes in the transcriptome, the translatome (ribosome footprints), the proteome, the metabolome and the physiological level are shown in red or blue color based on GO enrichment analysis. The description in red color displays upregulation after 2 h (normal type) or 4 h (boldface) of HL treatment; The description in blue color displays downregulation after 2 h (normal type) or 4 h (boldface) of HL treatment. Arrows indicate potential causal connections.

SUPPLEMENTAL INFORMATION

The following materials are available in the online version of this article.

Figure S1. HL treatment setup and time point selection.

Figure S2. Changes in electron transport in response to HL stress in maize and rice.

Figure S3. Quality control for the omics datasets generated in this study.

Figure S4. Significant changes detected in multi-omics studies.

Figure S5. Changes of GO pathways in response to high-light stress in maize and rice.

Figure S6. Quantitative analyses of HL stress-responsive genes associated with selected metabolic pathways in maize and rice.

Figure S7. Expression of heat shock protein genes (*HSP*) in response to HL treatment.

Figure S8. Cyclic electron flow, expression of D1 protein and xanthophyll cycle-related genes in maize and rice during 4 hours of HL stress.

Figure S9. Growth- and photosynthesis-related parameters in the maize *psbs* mutant and transgenic *PsbS* overexpression (*PsbS*-OE) lines.

Figure S10. Correlation networks of HL-responsive genes.

Figure S11. Changes in photosynthesis-related parameters upon HL treatment in wild-type rice plants (WT), *OsbZIP18* knockout (KO) lines and the *OsbZIP18* overexpression (OE) line.

Figure S12. Transcriptomic profiling of *OsbZIP18*-regulated HL responses.

Figure S13. ROS staining after HL treatment.

Figure S14. Changes in the expression of oxidative stress-related genes in maize and rice leaves after HL treatment.

Figure S15. Ratios of glycine to serine in rice and maize leaves during high light treatment.

Figure S16. Receiver operating characteristic (ROC) curves for machine learning models in maize.

Figure S17. Receiver operating characteristic (ROC) curves for machine learning models in rice.

Table S1. Number of differentially expressed units in each omics dataset.

Table S2. Read coverage in ORF.

Dataset S1. Genes with coordinated expression at the levels of transcription, translation and protein accumulation.

Dataset S2. Node genes in maize and rice correlation network.

Dataset S3. Node gene expression on different levels.

Dataset S4. HL-responsive transcription factors in maize and rice.

Dataset S5. Relative expression of genes in Cluster 9.

836 **REFERENCES**

837 **Anderson, C.M., Mattoon, E.M., Zhang, N.N., Becker, E., McHargue, W., Yang,**
838 **J.N., Patel, D., Dautermann, O., McAdam, S.A.M., Tarin, T., et al.** (2021). High
839 light and temperature reduce photosynthetic efficiency through different
840 mechanisms in the C4 model *Setaria viridis*. Commun. Biol. **4**:1092.

841 **Asada, K.** (2006). Production and scavenging of reactive oxygen species in
842 chloroplasts and their functions. Plant Physiol. **141**:391-396.

843 **Bassi, R., and Dall'Osto, L.** (2021). Dissipation of light energy absorbed in excess:
844 the molecular mechanisms. Annu. Rev. Plant. Biol. **72**:47-76.

845 **Bernacchi, C.J., Singsaas, E.L., Pimentel, C., Portis, A.R., and Long, S.P.** (2001).
846 Improved temperature response functions for models of Rubisco-limited
847 photosynthesis. Plant Cell Environ. **24**:253-259.

848 **Bhatnagar, A., Burman, N., Sharma, E., Tyagi, A., Khurana, P., and Khurana, J.P.**
849 (2023). Two splice forms of OsbZIP1, a homolog of AtHY5, function to regulate
850 skotomorphogenesis and photomorphogenesis in rice. Plant Physiol. **193**:426-447.

851 **Blatke, M.A., and Brautigam, A.** (2019). Evolution of C_4 photosynthesis predicted by
852 constraint-based modelling. Elife **8**:e49305.

853 **Brooks, M.D., Sylak-Glassman, E.J., Fleming, G.R., and Niyogi, K.K.** (2013). A
854 thioredoxin-like/β-propeller protein maintains the efficiency of light harvesting in.
855 Proc. Natl. Acad. Sci. U.S.A. **110**: E2733-E2740.

856 **Burman, N., Bhatnagar, A., and Khurana, J.P.** (2018). OsbZIP48, a HY5
857 transcription factor ortholog, exerts pleiotropic effects in light-regulated
858 development. Plant Physiol. **176**:1262-1285.

859 **Cazzaniga, S., Osto, L.D., Kong, S.G., Wada, M., and Bassi, R.** (2013). Interaction
860 between avoidance of photon absorption, excess energy dissipation and zeaxanthin
861 synthesis against photooxidative stress in *Arabidopsis*. Plant J. **76**:568-579.

862 **Chen, S., Songkumarn, P., Liu, J., and Wang, G.L.** (2009). A versatile zero
863 background T-vector system for gene cloning and functional genomics. Plant
864 Physiol. **150**:1111-1121.

865 **Christa, G., Cruz, S., Jahns, P., de Vries, J., Cartaxana, P., Esteves, A.C., Serôdio,**

J., and Gould, S.B. (2017). Photoprotection in a monophyletic branch of chlorophyte algae is independent of energy-dependent quenching (qE). New Phytol. **214**:1132-1144.

De Souza, A.P., Burgess, S.J., Doran, L., Hansen, J., Manukyan, L., Maryn, N., Gotarkar, D., Leonelli, L., Niyogi, K.K., and Long, S.P. (2022). Soybean photosynthesis and crop yield are improved by accelerating recovery from photoprotection. Science **377**:851-854.

Edelman, M., and Mattoo, A.K. (2008). D1-protein dynamics in photosystem II: the lingering enigma. Photosyn. Res. **98**:609-620.

Fernandez, O., Bethencourt, L., Quero, A., Sangwan, R.S., and Clement, C. (2010). Trehalose and plant stress responses: friend or foe? Trends Plant Sci. **15**:409-417.

Griffiths, C.A., Sagar, R., Geng, Y., Primavesi, L.F., Patel, M.K., Passarelli, M.K., Gilmore, I.S., Steven, R.T., Bunch, J., Paul, M.J., et al. (2016). Chemical intervention in plant sugar signalling increases yield and resilience. Nature **540**:574-578.

Hoagland, D.R., and Arnon, D.I. (1950). The water-culture method for growing plants without soil. In California Agricultural Experiment Station, (University of California, Berkeley: Baltimore, USA), p 32.

Huang, J., Zhao, X., and Chory, J. (2019). The *Arabidopsis* transcriptome responds specifically and dynamically to high light stress. Cell Rep. **29**:4186-4199.e4183.

Ishikawa, N., Takabayashi, A., Noguchi, K., Tazoe, Y., Yamamoto, H., von Caemmerer, S., Sato, F., and Endo, T. (2016). NDH-mediated cyclic electron flow around photosystem I is crucial for C_4 photosynthesis. Plant and Cell Physiol. **57**:2020-2028.

Jiang, X.C., Xu, J., Lin, R., Song, J.N., Shao, S.J., Yu, J.Q., and Zhou, Y.H. (2020). Light-induced HY5 functions as a systemic signal to coordinate the photoprotective response to light fluctuation. Plant Physiol. **184**:1181-1193.

Karpinski, S., Reynolds, H., Karpinska, B., Wingsle, G., Creissen, G., and Mullineaux, P. (1999). Systemic signaling and acclimation in response to excess excitation energy in *Arabidopsis*. Science **284**:654-657.

Kim, E., Watanabe, A., Duffy, C.D.P., Ruban, A.V., and Minagawa, J. (2020). Multimeric and monomeric photosystem II supercomplexes represent structural adaptations to low- and high-light conditions. J. Biol. Chem. **295**:14537-14545.

Krause, G.H. (1988). Photoinhibition of photosynthesis. An evaluation of damaging and protective mechanisms. Physiol. Plantarum **74**:566-574.

Krause, G.H., and Weis, E. (1991). Chlorophyll fluorescence and photosynthesis: the basics. Annu. Rev. Plant Physiol. Plant Mol. Biol. **42**:313-249.

Krause, G.H., Vernotte, C., and Briantais, J.M. (1982). Photoinduced quenching of chlorophyll fluorescence in intact chloroplasts and algae. Resolution into two components. Biochim. Biophys. Acta Bioenerg. **679**:116-124.

Kress, E., and Jahns, P. (2017). The dynamics of energy dissipation and xanthophyll conversion in *Arabidopsis* indicate an indirect photoprotective role of zeaxanthin in slowly inducible and relaxing components of non-photochemical quenching of excitation energy. Front. Plant Sci. **8**:2094.

Kretzschmar, T., Pelayo, M.A.F., Trijatmiko, K.R., Gabunada, L.F.M., Alam, R., Jimenez, R., Mendioro, M.S., Slamet-Loedin, I.H., Sreenivasulu, N., Bailey-Serres, J., et al. (2015). A trehalose-6-phosphate phosphatase enhances anaerobic germination tolerance in rice. Nat. Plants **1**:15124.

Krishnan-Schmieden, M., Konold, P.E., Kennis, J.T.M., and Pandit, A. (2021). The molecular pH-response mechanism of the plant light-stress sensor PsbS. Nat. Commun. **12**:2291.

Kromdijk, J., Glowacka, K., Leonelli, L., Gabilly, S.T., Iwai, M., Niyogi, K.K., and Long, S.P. (2016). Improving photosynthesis and crop productivity by accelerating recovery from photoprotection. Science **354**:857-861.

López-Calcagno, P.E., Abuzaid, A.O., Lawson, T., and Raines, C.A. (2017). *Arabidopsis* CP12 mutants have reduced levels of phosphoribulokinase and impaired function of the Calvin-Benson cycle. J. Exp. Bot. **68**:2285-2298.

Li, L., Aro, E.M., and Millar, A.H. (2018). Mechanisms of photodamage and protein turnover in photoinhibition. Trends Plant Sci. **23**:667-676.

Li, L., Duncan, O., Ganguly, D.R., Lee, C.P., Crisp, P.A., Wijerathna-Yapa, A.,

926 **Salih, K., Trösch, J., Pogson, B.J., and Millar, A.H.** (2022). Enzymes degraded
927 under high light maintain proteostasis by transcriptional regulation in *Arabidopsis*.
928 Proc. Natl. Acad. Sci. U.S.A. **119**: e2121362119.
929 **Li, X., Wang, P., Li, J., Wei, S., Yan, Y., Yang, J., Zhao, M., Langdale, J.A., and**
930 **Zhou, W.** (2020). Maize GOLDEN2-LIKE genes enhance biomass and grain
931 yields in rice by improving photosynthesis and reducing photoinhibition. Commun.
932 Biol. **3**:151.
933 **Liang, C., Cheng, S.F., Zhang, Y.J., Sun, Y.Z., Fernie, A.R., Kang, K., Panagiotou,**
934 **G., Lo, C., and Lim, B.L.** (2016). Transcriptomic, proteomic and metabolic
935 changes in leaves after the onset of illumination. BMC Plant Biol. **16**: 43.
936 **Long, S.P., and Bernacchi, C.J.** (2003). Gas exchange measurements, what can they
937 tell us about the underlying limitations to photosynthesis? Procedures and sources
938 of error. J. Exp. Bot. **54**:2393-2401.
939 **Long, S.P., Humphries, S., and Falkowski, P.G.** (1994). Photoinhibition of
940 photosynthesis in nature. Annu. Rev. Plant Physiol. Plant Mol. Biol. **45**:633-662.
941 **Malnoë, A., Schultink, A., Shahrasbi, S., Rumeau, D., Havaux, M., and Niyogi,**
942 **K.K.** (2018). The plastid lipocalin LCNP is required for sustained photoprotective
943 energy dissipation in *Arabidopsis*. Plant Cell **30**:196-208.
944 **Mao, Y., Zhang, H., Xu, N., Zhang, B., Gou, F., and Zhu, J.K.** (2013). Application
945 of the CRISPR-Cas system for efficient genome engineering in plants. Mol. Plant
946 **6**:2008-2011.
947 **McMurtrie, R.E., and Wang, Y.P.** (1993). Mathematical models of the photosynthetic
948 response of tree stands to rising CO_2 concentrations and temperatures. Plant Cell
949 Environ. **16**:1-13.
950 **Mittler, R., Zandalinas, S.I., Fichman, Y., and Van Breusegem, F.** (2022). Reactive
951 oxygen species signalling in plant stress responses. Nat. Rev. Mol. Cell Bio.
952 **23**:663-679.
953 **Moroney, J.V., Jungnick, N., DiMario, R.J., and Longstreth, D.J.** (2013).
954 Photorespiration and carbon concentrating mechanisms: two adaptations to high
955 O_2, low CO_2 conditions. Photosyn. Res. 117:121-131.

Munekage, Y.N., and Taniguchi, Y.Y. (2016). Promotion of cyclic electron transport around photosystem I with the development of C_4 photosynthesis. Plant Cell Physiol. **57**:897-903.

Nilkens, M., Kress, E., Lambrev, P., Miloslavina, Y., Muller, M., Holzwarth, A.R., and Jahns, P. (2010). Identification of a slowly inducible zeaxanthin-dependent component of non-photochemical quenching of chlorophyll fluorescence generated under steady-state conditions in *Arabidopsis*. Biochim. Biophys. Acta. Bioenerg. **1797**:466-475.

Nishiyama, Y., Allakhverdiev, S.I., and Murata, N. (2006). A new paradigm for the action of reactive oxygen species in the photoinhibition of photosystem II. Biochim. Biophys. Acta. Bioenerg. **1757**:742-749.

Niyogi, K.K., Grossman, A.R., and Bjorkman, O. (1998). *Arabidopsis* mutants define a central role for the xanthophyll cycle in the regulation of photosynthetic energy conversion. Plant Cell **10**:1121-1134.

Ort, D.R. (2001). When there is too much light. Plant Physiol. **125**:29-32.

Paul, M.J., Gonzalez-Uriarte, A., Griffiths, C.A., and Hassani-Pak, K. (2018). The Role of trehalose 6-phosphate in crop yield and resilience. Plant Physiol. **177**:12-23.

Raven, J.A. (2011). The cost of photoinhibition. Physiol. Plantarum **142**:87-104.

Schuster, M., Gao, Y., Schottler, M.A., Bock, R., and Zoschke, R. (2020). Limited responsiveness of chloroplast gene expression during acclimation to high light in tobacco. Plant Physiol. **182**:424-435.

Shi, Y.F., Ke, X.S., Yang, X.X., Liu, Y.H., and Hou, X. (2022). Plants response to light stress. J. Genet. Genomics **49**:735-747.

Slattery, R.A., Walker, B.J., Weber, A.P.M., and Ort, D.R. (2018). The impacts of fluctuating light on crop performance. Plant Physiol. **176**:990-1003.

Sonoike, K. (2011). Photoinhibition of photosystem I. Physiol. Plantarum **142**:56-64.

Sun, Y., Wang, B., Ren, J., Zhou, Y., Han, Y., Niu, S., Zhang, Y., Shi, Y., Zhou, J., Yang, C., et al. (2022). OsbZIP18, a positive regulator of serotonin biosynthesis, negatively controls the UV-B tolerance in rice. Int. J. Mol. Sci. **23**:3215.

Szalai, G., Kellos, T., Galiba, G., and Kocsy, G. (2009). Glutathione as an antioxidant and regulatory molecule in plants under abiotic stress conditions. J. Plant Growth Regul. **28**:66-80.

Takahashi, S., and Badger, M.R. (2011). Photoprotection in plants: a new light on photosystem II damage. Trends Plant Sci. **16**:53-60.

von Caemmerer, S. (2021). Updating the steady-state model of C_4 photosynthesis. J. Exp. Bot. **72**:6003-6017.

Xing, H.L., Dong, L., Wang, Z.P., Zhang, H.Y., Han, C.Y., Liu, B., Wang, X.C., and Chen, Q.J. (2014). A CRISPR/Cas9 toolkit for multiplex genome editing in plants. BMC Plant Biol. **14**:327.

Yabiku, T., and Ueno, O. (2019). Structural and photosynthetic re-acclimation to low light in C_4 maize leaves that developed under high light. Ann. Bot. **124**:437-445.

Yamamoto, Y., Aminaka, R., Yoshioka, M., Khatoon, M., Komayama, K., Takenaka, D., Yamashita, A., Nijo, N., Inagawa, K., Morita, N., et al. (2008). Quality control of photosystem II: impact of light and heat stresses. Photosyn. Res. **98**:589-608.

Yoshida, S., Forno, D.A., Cock, J.H., and Gomez, K.A. (1976). Routine procedure for growing rice plants in culture solution. In Laboratory manual for physiological studies of rice, (The International Rice Research Institute: Laguna, Philippines), pp. 46-49.

Zhang, Y.J., and Fernie, A.R. (2018). On the role of the tricarboxylic acid cycle in plant productivity. J. Integr. Plant Biol. 60:1199-1216.